



Long-term corrosion behaviour of stainless reinforcing steel in mortar exposed to chloride environment

Marijana Serdar^{a,*}, Lidija Valek Žulj^b, Dubravka Bjegović^a

^a Department of Materials, Faculty of Civil Engineering, University of Zagreb, HR-10000 Zagreb, Croatia

^b Department of Electrochemistry, Faculty of Chemical Engineering and Technology, University of Zagreb, HR-10000 Zagreb, Croatia

ARTICLE INFO

Article history:

Received 19 September 2012

Accepted 26 November 2012

Available online 3 December 2012

Keywords:

A. Stainless steel

B. Concrete

C. EIS

D. Passivity

E. Pitting corrosion

ABSTRACT

Long-term corrosion behaviour of six stainless reinforcing steels embedded in mortar and exposed to chloride media was monitored by electrochemical impedance spectroscopy at the open circuit potential during the period of 2 years. Corrosion behaviour of studied steels was divided into two phases characterized by different interfacial behaviour: (i) passive phase and (ii) pitting propagation phase. After 2 years, duplex steel 1.4362 showed very good corrosion performance similar to austenitic steel 1.4401. Steel types with low Ni content but with high N and Mn content, 1.4597 and 1.4162, showed lower corrosion resistance compared to austenitic steel 1.4301.

© 2012 Elsevier Ltd. All rights reserved.

1. Introduction

Inspections of reinforced concrete structures exposed to aggressive (marine or continental) environment have shown that almost all of them have degraded due to chloride induced corrosion of reinforcement and that corrosion is the main reason for their reduced service life [1]. One of the methods to prolong corrosion initiating and consequently service life of reinforced concrete structure is the use of stainless steels as a substitution of part or complete reinforcement in concrete [2]. Until recently, most of the published literature on the use of stainless steels as reinforcement has been focused on austenitic stainless steel types, 1.4301 and 1.4401, showing their very good corrosion behaviour in laboratory studies [3–5] and application in structures [6,7]. However, due to their cost induced by high content of Ni and Mo, search for more economical novel stainless reinforcing steels has been a subject of recent studies [8–15]. Since the price of these steels is more comparable to the price of common black steel reinforcement than the price of highly alloyed stainless steels, the idea of using lower alloyed stainless steel as reinforcement is economically justified. Studies investigating the corrosion behaviour of different types of steel are mostly based on testing in pore solution simulating concrete, either aiming at identifying the passivity of these steels [4,11,16,17] or environmental conditions leading to corrosion initiation [5,10,18,19]. Although electrochemical meth-

ods in simulated condition are valuable tool for comparison and elimination of different types of steel due to a high reproducibility of experiment, the results of such investigations should be confirmed by the long-term investigation in concrete. The experimental setup of electrochemical tests in simulated pore solution cannot reproduce a numerous conditions that are really present in concrete, like inhomogeneity of the steel/concrete interface, possible processes in crevices, lower conductivity of electrolyte, limited oxygen diffusion rate, etc. Giving the above reasons, investigation of potent steels in pore solution give valuable information on passivity and initiation of corrosion, but long-term monitoring of the behaviour of these types of steel in concrete during propagation of natural corrosion are of great importance in confirmation of the results [20–22].

The aim of this study was to investigate long-term corrosion behaviour of different types of corrosion resistant steels embedded in mortar and exposed to simulated aggressive marine environment by employing the electrochemical impedance spectroscopy (EIS) at the open circuit potential (E_{OC}). Till now EIS measurements have been successfully used to determine corrosion resistance of steel in pore solution and in mortar [12,23–25] and also to investigate the influence of different admixtures on the concrete properties [26–28]. In the present study EIS measurements were used to monitor and analyse behaviour of stainless reinforcing steel in mortar during passivity, initiation of localized corrosion, and propagation of corrosion process. Six different types of steel were studied in order to confirm numerous experimental results in simulated pore solutions on their corrosion performance for concrete reinforcement application, that are available in literature.

* Corresponding author. Tel.: +385 14639118; fax: +385 4597118.

E-mail addresses: mserdar@grad.hr (M. Serdar), lvalek@fkit.hr (L.V. Žulj), dubravka@grad.hr (D. Bjegović).

2. Materials and methods

Six different types of steel reinforcement were chosen based on the content of key elements such as nickel, chromium, molybdenum and manganese. Two types of low-Ni steels, ferritic (1.4003) and austenitic steel (1.4597), one type of low-Ni lean duplex steel (1.4162), two austenitic stainless steels (1.4301 and 1.4401) and one duplex steel (1.4362) were tested. All chosen and tested steels were corrugated rebars, produced as concrete reinforcement. The surface of steels was not changed nor controlled before the testing, and all steels were tested with the as-received state of the surface. The chemical compositions of tested reinforcing steels together with PREN (pitting resistance equivalent number) are given in Table 1. PREN is calculated from chemical composition of steel, for ferritic and austenitic stainless steel according to Eq. (1) [2]:

$$\text{PREN}_{16} = \text{wt}\% \text{Cr} + 3.3 \times \text{wt}\% \text{Mo} + 16 \times \text{wt}\% \text{N} \quad (1)$$

For duplex steels PREN is calculated according to Eq. (2):

$$\text{PREN}_{30} = \text{wt}\% \text{Cr} + 3.3 \times \text{wt}\% \text{Mo} + 30 \times \text{wt}\% \text{N} \quad (2)$$

Mortar was prepared using Portland cement without mineral admixture with 0.7 water/cement ratio. Crushed limestone with a maximum particle size of 4 mm was chosen as an aggregate. Mortar mixture was specifically designed to produce a low quality mortar to ensure that corrosion will naturally occur in the reinforced mortar samples exposed to a simulated aggressive marine environment during a reasonable time of exposure. Prepared fresh mortar was poured into \varnothing 40 mm \times 140 mm plastic moulds that had reinforcing steel rebar placed in the middle ($d = 14$ mm for all steels except 1.4162 with $d = 12$ mm and 1.4401 with $d = 10$ mm; $l = 10$ cm for all steels). For each type of steel 3 reinforced mortar samples were prepared (Fig. 1.). The preparation of samples was conducted in the manner that assures the reproducibility of the conditions to which the rebar was exposed, in order to achieve that all the rebar was exposed to as much as possible similar corrosive environment. Beside samples for corrosion investigation, set of samples for testing mortar mechanical and durability properties were also prepared. All samples were cured in a humidity chamber, with controlled humidity (95% RH) and temperature (20 ± 2 °C), for 28 days. After curing, samples for corrosion investigation were partially submerged into 3.5 wt.% NaCl solution (0.6 mol dm^{-3}). Level of aggressive sodium solution was 70 mm,

with lower half of the sample submerged into the solution, and upper half exposed to air. The oxygen penetration was expected to proceed from the upper part of the sample and the chloride penetration from the submerged part of the specimen. All the samples were treated in the same manner in order to achieve as much as possible similar conditions to which the steel rebar was exposed. Results of testing physical, mechanical and durability properties of mortar are presented in Table 2. It can be seen that prepared mortar, regardless satisfying strength, has a poor resistance to penetration of aggressive substances (high water and gas permeability coefficient, and high apparent chloride diffusion coefficient).

Electrochemical impedance spectroscopy (EIS) measurements were performed using PAR VMP2 potentiostat/galvanostat with VMP3/Z impedance option. Standard three electrode system was used, with titanium mesh as a counter electrode, saturated calomel electrode (SCE) as a reference electrode, and aforementioned reinforced mortar samples as a working electrode. All the potentials presented are expressed vs. SCE. E_{OC} and EIS spectra were measured periodically during the exposure in order to monitor and analyse behaviour of different types of steel in mortar exposed to aggressive environment. Measurements were periodically repeated after 1, 2, 3, 4, 6 and 24 months of exposure. EIS measurements were performed in the frequency range between 100 kHz and 0.1 mHz at the E_{OC} with *ac* perturbation ± 10 mV.

Micrographs were taken with the Zeiss EVO SEM equipped with an EDAX EDS detector in EPS of UC Berkeley. SEM was operating in backscatter mode, at an accelerating voltage of 15 kV for imaging, with a magnification in the range of 60–160 \times and the probe current around 2 nA.

3. Results and discussion

In order to characterize corrosion behaviour of the reinforcing stainless steel embedded into the mortar (Fig. 1) and exposed to the chloride media, before and after the pitting initiation, EIS spectra were measured after different exposure times at the E_{OC} . Three representative sets of EIS spectra after 1 and 24 months of exposure to 3.5 wt.% NaCl solution are presented in Fig. 2; mortar samples reinforced with low-Ni ferritic steel 1.4003 (a), low-Ni duplex steel 1.4162 (b) and duplex steel 1.4362 (c). The data measured for other steels that are not presented here showed similar behaviour. At high frequencies (higher than 10^2 Hz), impedance module,

Table 1
Chemical composition of tested steel grades.

Steel grade		PREN	Chemical composition, wt.%										
EN 10088-1	AISI		C	Si	Mn	P	S	N	Cr	Cu	Mo	Ni	Fe
1.4003	410	12.42	0.018	0.80	0.56	0.013	<0.001	0.01	12.37	0.02	0.02	0.46	Bal.
1.4597	204Cu	21.78	0.038	0.42	7.94	0.021	0.005	0.15	16.23	2.14	0.32	2.11	Bal.
1.4162	2101	23.41	0.045	0.67	5.28	0.000	0.001	0.20	19.88	0.23	0.10	1.22	Bal.
1.4301	304	19.87	0.058	0.42	1.46	0.019	<0.001	0.05	18.24	0.11	0.04	7.93	Bal.
1.4362	2304	24.26	0.020	0.58	1.09	0.022	<0.001	0.07	22.22	0.28	0.28	3.57	Bal.
1.4401	316	27.70	0.027	0.35	1.98	0.034	0.002	0.11	15.82	0.40	2.60	12.33	Bal.

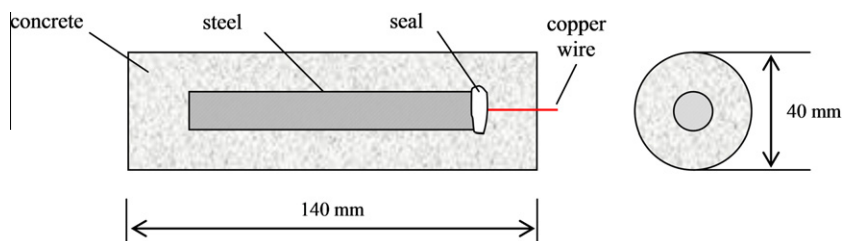


Fig. 1. Schematic view of the reinforced mortar sample used as a working electrode in electrochemical tests.

Table 2
Properties of mortar used for preparation of specimens.

Property	Standard	Value
Density, kg/dm ³	HRN EN 12350-6:2000	2.35
Porosity, %	HRN EN 12350-7:2000	2.7
Compressive strength, MPa	HRN EN 12390-3:2002	32.7
Tensile strength, MPa	HRN EN 12390-5:2001 + AC:2005	5.2
Modulus of elasticity, GPa	HRN U.M1.025:1982	27.3
Water permeability, m/s	HRN EN 12390-8:2001	1.5×10^{-10}
Apparent chloride diffusion coefficient, m ² /s	NT BUILD 492, 1999-11	20×10^{-12}
Gas permeability coefficient, m ²	CEMBUREAU RILEM TC 116	1.3×10^{-16}

$\log|Z|$ vs. *Frequency* plot exhibits a slope close to zero while the phase angle approaches 0° reflecting the resistance of mortar (bulk material and pore solution). At intermediate frequencies (between 10² Hz and 10⁻² Hz), the $\log|Z|$ vs. *Frequency* plot has a slope close to -1 and the phase angle close to -80° showing the capacitive behaviour at the rebar/mortar interface. At low frequencies (between 10⁻² Hz and 10⁻⁴ Hz) a plateau in $\log|Z|$ vs. *Frequency* is observed with the phase angle decreasing towards 0°, where resistance to the charge-transfer processes is reflected. Repeated measurements during 2 years of exposure of samples to the chloride media, revealed increase of impedance module at high and low frequencies reflecting the enhancement of the electrolyte and interfacial resistance while capacitance phase angle gradually decreased due to the inhomogeneity of the steel surface induced by the growth of the passive film. Interfacial behaviour of steels embedded in mortar during 2 year exposure to chloride media could be divided into two phases: (i) passive phase or pitting initiation phase characterized by the enhancement of interfacial resistances and (ii) after the pitting appearance, pitting propagation phase characterized by the decrease of interfacial resistances and increase of interfacial capacitance.

3.1. Analysis of EIS spectra during passivity and after the pitting initiation

The first period, before the pitting appearance, is usually characterised by the enhancement of the corrosion resistance of stainless steel through growth and change of the chemical composition of passive film [16,17]. EIS spectra, obtained for the tested stainless steels embedded in mortar and exposed to the chloride media (Fig. 2.), were fitted to the equivalent electrical circuit presented in Fig. 3 and the resulting parameters are presented in Tables 3–5. In the proposed circuit frequency-dependent constant-phase element (CPE) was introduced instead of a pure capacitance (C), to account for the inhomogeneities present at the steel surface/pore structure interface. The fitting procedure also showed a better agreement between theoretical and experimental data when CPE was introduced. The impedance of a constant-phase element is defined as $Z_{CPE} = [CPE(j\omega)^n]^{-1}$ [29]. The deviation of CPE from pure capacitance is characterized by its exponent n . For pure capacitance $n = 1$, and with an increase in capacitance dispersion, n decreases [24,29]. Using the constant-phase element values, CPE, the exponent n , the resistance of the electrolyte R_{el} and the resistance R_1 , the capacitance value, C_1 , can be calculated using the Eq. (3) [29]:

$$C_1 = \left[\frac{CPE}{(R_{el}^{-1} + R_1^{-1})^{(n-1)}} \right]^{1/n} \quad (3)$$

The accuracy of fitting is illustrated on all diagrams showing impedance spectra (Figs. 2a–c and 6a–b), with experimental values presented in symbols and fitted values in lines (fitting error was under 10% for all obtained parameters).

Physical meaning of the elements in the proposed equivalent electrical circuit is depicted according to the schematic view of the interface. R_{mortar} , corresponding to the high frequency response, represents the mortar bulk resistance, being in the particular samples used in this investigation the resistance of mortar and the electrolyte resistance that is negligible compared to the mortar resistance. During early times of exposure, between 1 and 4 months, values of mortar resistance, R_{mortar} , of all tested samples increased over time (Tables 3–5.) probably due to the hydration process and creation of less porous cement matrix during aging [26,27]. After significant time of exposure, this resistance started to decrease probably due to the increase of chloride content inside the cement matrix, which made the mortar more conductive. Significant variations in mortar resistance during time are even more pronounced due to the poor quality of mortar, causing easy penetration of solution inside the sample and crystallisation of salt inside the mortar pore structure. When the steel samples are embedded in mortar spectra in high-frequency domain cannot be interpreted in the same manner as the spectra obtained in the solution. Due to the inhomogeneity of the mortar and charge distribution in the interfacial transition zone between the aggregate and the cement paste and between the steel surface and non-homogeneous bulk cement surrounding it may induce non-ideal EIS response more complex from the ones in solution [27,28]. Some of the more complicated spectra at high frequency are for example evident in the case of longer exposure of steel 1.4003 (Fig. 2a). In the present study, high-frequency domain was not analysed in detail, since the main focus of the research was on the low frequency behaviour of different types of steel in mortar.

During the passivity period, the second time constant parameters appearing at the low frequencies (R_2 , C_2 and n_2 in Table 3–5 and Fig. 3a) were attributed to the non-ideal interfacial capacitance of the steel surface and charge transfer resistance that reflects the corrosion resistance of the steel surface controlled by the properties of passive film [12,13]. The first time constant parameters appearing at the intermediate frequencies (R_1 , C_1 , n_1 in Tables 3–5 and Fig. 3a) seem to be related with a redox transformation of the corrosion products that occurs on the surface of the oxide film [12,25]. The existence of two time constants at the presented impedance spectra is not always clearly evident, but fitting data with parallel distributed equivalent electrical circuit was necessary in order to obtain the results with satisfying accuracy. The superposition of the two time constants is common in the EIS results obtained at the interface with thin film what makes it hard to distinguish between the properties of the passive film/electrolyte interface and the passive film. The presence of the two overlapped time constants could be observed from the slight asymmetry of the phase angle maximum towards the low frequencies. The values of C_1 and R_1 determined at the intermediate frequencies show significant oscillation due to the limitations in spectra analysis induced by overlapment of the peaks. R_1 values are similar for all tested steels and are significantly lower compared to the R_2 for all the samples.

Looking at the trend of the resistance R_2 and capacitance C_2 values for steel 1.4162 and 1.4362 presented in Tables 4 and 5 it can be observed that charge transfer resistance and interfacial capacitance increased at the beginning of the exposure. Such behaviour can be attributed to the formation of passive film on the steel surface that is more resistant to corrosion with time [12]. Additionally, the growth of the passive film induced an enhancement of the surface roughness that increased the area at which the double layer formed, thus resulting in an increase of the capacitance calculated

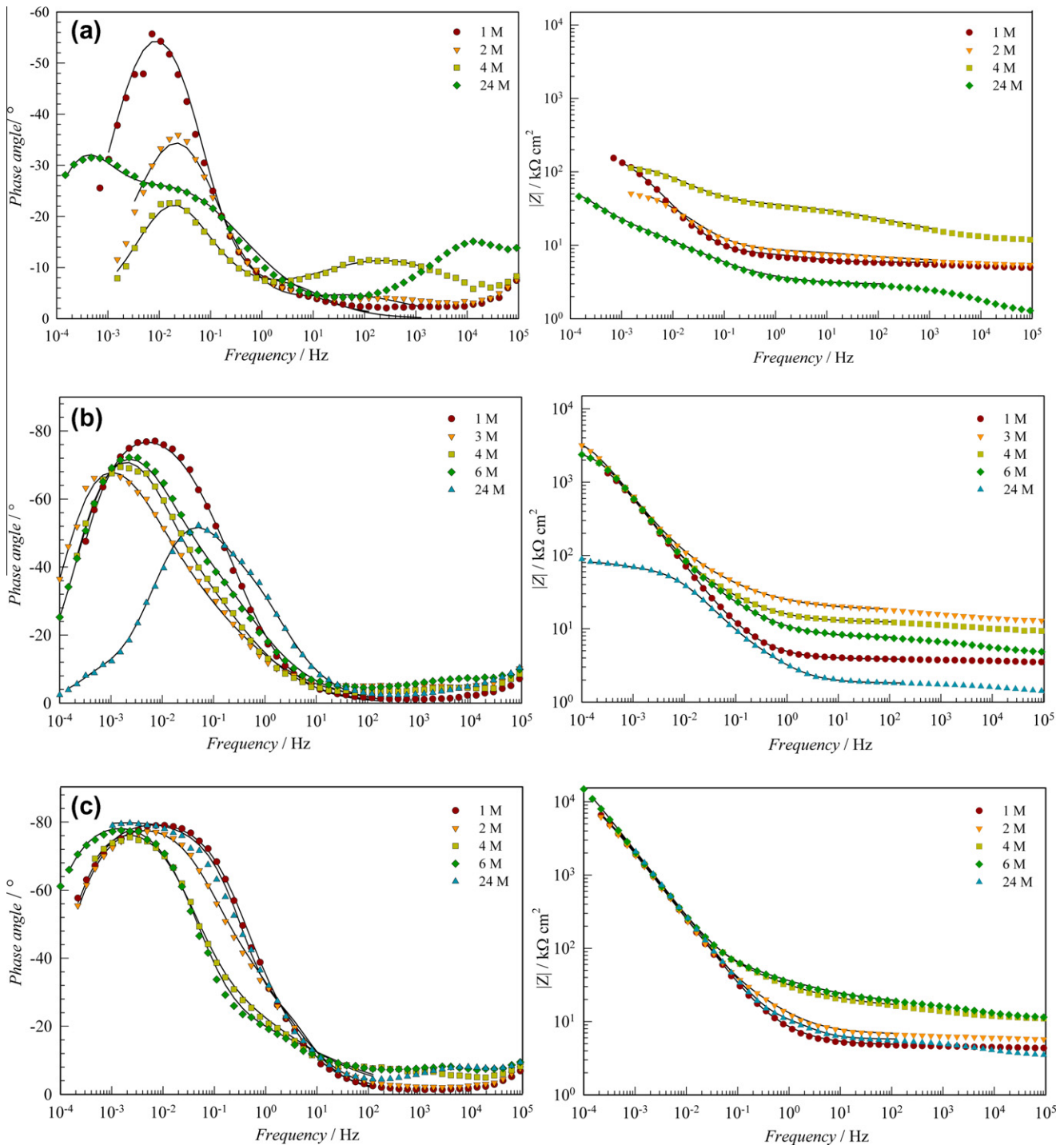


Fig. 2. Bode plots of mortar samples reinforced with 1.4003 steel (a), 1.4162 steel (b) and 1.4362 steel (c), after different times of exposure to 3.5 wt.% NaCl solution (experimental values given in dots, fitted in lines).

towards the geometrical surface area of the electrode. The values of the charge transfer resistance, R_2 were between 2 and 30 $\text{M}\Omega \text{ cm}^2$, which is significantly higher than the values for black steel reinforcement, but in the range of values found for stainless steels in pore solution [11,12]. High resistance at the interface and good corrosion resistance properties of stainless steel have been attributed to the inner layer of the passive film, enriched with Cr, Ni and Mo [3,16,17]. This would be in agreement with the model of passive film formation and growth on stainless steel in alkaline solution, suggested by Addari et al. [16]. According to their XPS results, the inner layer of the passive film formed on stainless steel is

mainly formed of Cr(III) oxy-hydroxide, while the outer layer is mainly composed of Fe(III) oxy-hydroxide. As seen in Fig. 2b and c and also Tables 4 and 5, in the initial phase a passive film resistance enhanced with time. After certain time of exposure resistant and stable film was formed and both resistance and capacitance did not change significantly over time (4 and 6 months of exposure for steel 1.4162 and 1.4362).

Looking at the trend of interfacial resistance R_2 and capacitance C_2 values (Tables 3–5), it could be observed that after a certain time of exposure the resistances started to decline. A significant decrease of the interfacial resistance followed by an increase of the

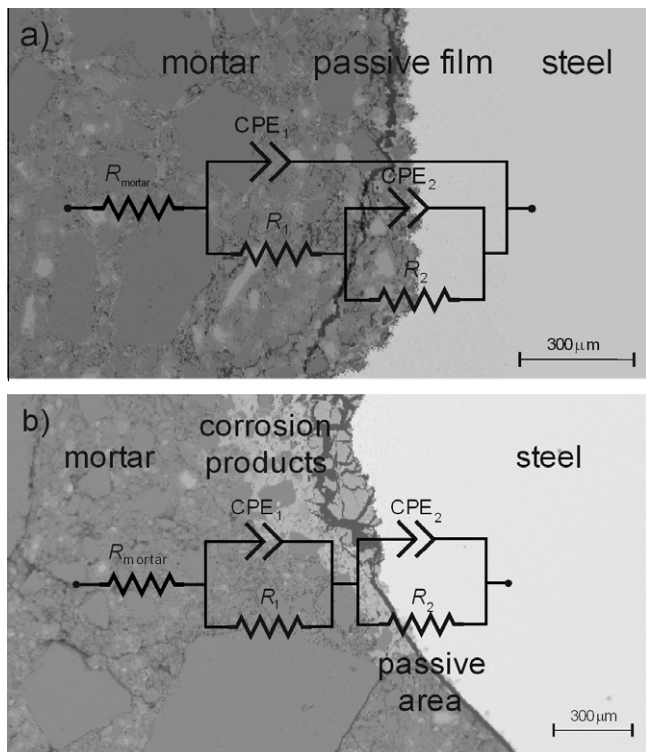


Fig. 3. Equivalent electrical circuit reflecting the phenomena at the interface before the pitting initiation shown on SEM image of steel 1.4162/mortar interface after 24 months of exposure (a); and after the pitting initiation shown on SEM image of steel 1.4003/mortar interface after 24 months of exposure (b).

interfacial capacitance could be observed for steel 1.4003 after 4 months of exposure and for steel 1.4162 after 24 month. Such results may be an indicator of the initiation of pitting corrosion, i.e.

the change of the steel surface from passive state to pitting corrosion. The period after the pitting appearance is usually characterized by the local accumulation of corrosion products induced by the pitting propagation [1]. A new phenomenon at the interface generated new time constant at the intermediate frequencies of the EIS spectra reflecting the properties of the corrosion products formed at the steel surface (Fig. 3b). The spectra could be fitted to the equivalent electrical circuit presented in Fig. 3b. The first time constant was attributed to the properties of the corrosion products layer formed at the pitted surface (C_1 and R_1 in Tables 3–5 and in Fig. 3b) while the second time constant was attributed to the sum of processes appearing at the pitted and passive area (C_2 and R_2 in Tables 3–5 and in Fig. 3b) [24,25,30].

A significant increase in the capacitance C_1 and C_2 observed in the case of steel 1.4003, Table 3, was attributed to the formation of a rough layer of corrosion products covering the pitted surface (Fig. 2a, Table 3). These capacitances are several mF cm^{-2} high, which is significantly higher than the double-layer capacitance of the passive steel [11,25]. A similar increase in capacitance during pitting propagation was obtained in our previous research performed in the solution [24]. Similar behaviour could also be found in the literature in the case of corroded carbon steel reinforcement in concrete after long-term exposure to aggressive environment [23]. After the pitting initiation, a new time constant appeared at the intermediate frequencies with capacitive response with very low n value typical of porous layers. Therefore, it can be assumed that the corrosion products formed by the pitting corrosion are porous and that the significant increase of the double layer capacitance after the pitting initiation can be ascribed to the enhancement of the surface roughness induced by the pitting and corrosion product accumulation.

In the case of steel 1.4162 (Fig. 2b, Table 4) the intermediate – frequency impedance response of the corrosion products and decrease of interfacial resistance after 2 years of exposure to chloride media could be observed. These spectra show a third time

Table 3

EIS parameters obtained by fitting the impedance spectra for mortar samples reinforced with 1.4003 after different exposure times (Fig. 2a).

Exposure time, months	E_{oc}/V_{SCE}	$R_{mortar}/k\Omega \text{ cm}^2$	$R_1/k\Omega \text{ cm}^2$	$C_1/\mu\text{F cm}^{-2}$	n_1	$R_2/k\Omega \text{ cm}^2$	$C_2/\mu\text{F cm}^{-2}$	n_2
1	-0.318	5.6	2.3	26.8	0.75	182.2	516.5	0.85
2	-0.361	5.8	2.6	1.6	0.51	57.7	431.2	0.76
4	-0.325	10.3	27.6	0.1	0.39	86.9	230.0	0.73
24	-0.496	2.8	16.7	1980.0	0.51	55.5	24683.1	0.80

Table 4

EIS parameters obtained by fitting the impedance spectra for mortar samples reinforced with 1.4162 after different exposure times (Fig. 2b).

Exposure time, months	E_{oc}/V_{SCE}	$R_{mortar}, k\Omega \text{ cm}^2$	$R_1, k\Omega \text{ cm}^2$	$C_1, \mu\text{F cm}^{-2}$	n_1	$R_2, k\Omega \text{ cm}^2$	$C_2, \mu\text{F cm}^{-2}$	n_2			
1	-0.164	3.9	16.2	109.8	0.88	2570.0	77.8	0.96			
3	-0.158	18.9	72.1	50.6	0.70	4193.1	135.5	0.91			
4	-0.100	12.2	37.0	159.1	0.57	2772.5	286.0	0.94			
6	-0.130	7.5	33.0	178.5	0.57	2716.1	282.6	0.94			
24	-0.392	1.8	28.0	210.7	0.73	$R_2, k\Omega \text{ cm}^2$ 55.3	$R_3, k\Omega \text{ cm}^2$ 24.0	$C_2, \mu\text{F cm}^{-2}$ 91.3	$C_3, \mu\text{F cm}^{-2}$ 698.9	n_2 0.85	n_3 0.59

Table 5

EIS parameters obtained by fitting the impedance spectra for mortar samples reinforced with 1.4362 after different exposure times (Fig. 2c).

Exposure time, months	E_{oc}/V_{SCE}	$R_{mortar}/k\Omega \text{ cm}^2$	$R_1/k\Omega \text{ cm}^2$	$C_1/\mu\text{F cm}^{-2}$	n_1	$R_2/k\Omega \text{ cm}^2$	$C_2/\mu\text{F cm}^{-2}$	n_2
1	-0.165	4.7	9.8	21.7	0.88	15384.0	36.4	0.92
2	-0.167	6.7	28.3	19.0	0.83	15999.6	36.9	0.95
4	-0.108	12.6	59.6	36.1	0.45	14170.1	109.1	0.92
6	-0.097	14.2	47.4	14.8	0.45	33338.5	118.4	0.91
24	-0.147	4.5	5.9	37.7	0.60	37276.3	118.8	0.91

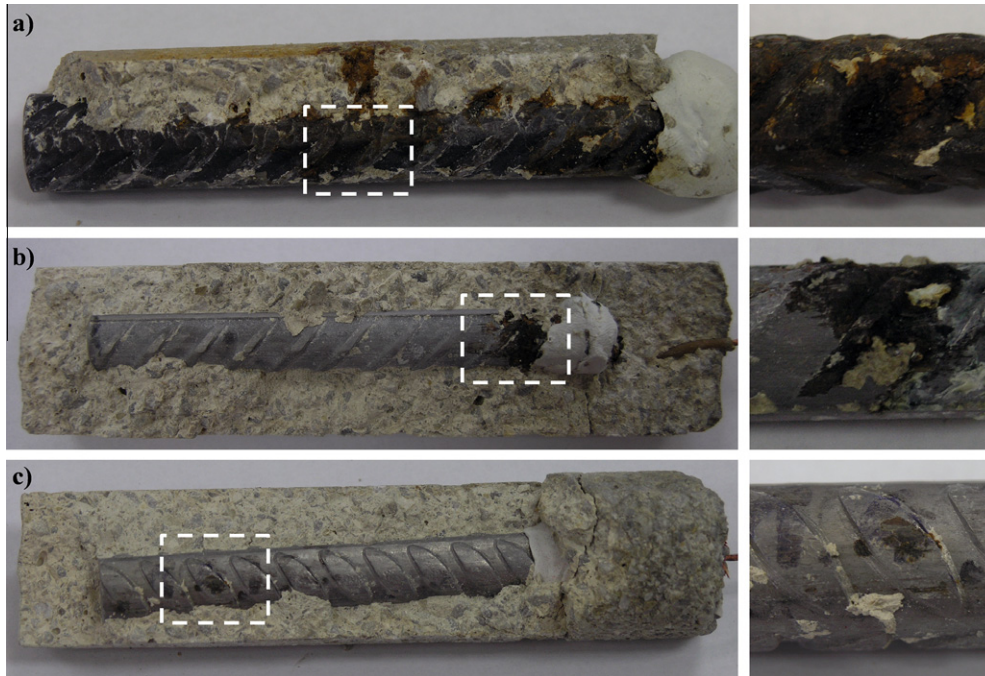


Fig. 4. Appearance of the samples after 24 months of exposure to 3.5 wt.% NaCl solution on the left, with enlarged corrosion attack on the right side: steel 1.4003 (a), steel 1.4162 (b), steel 1.4362 (c).

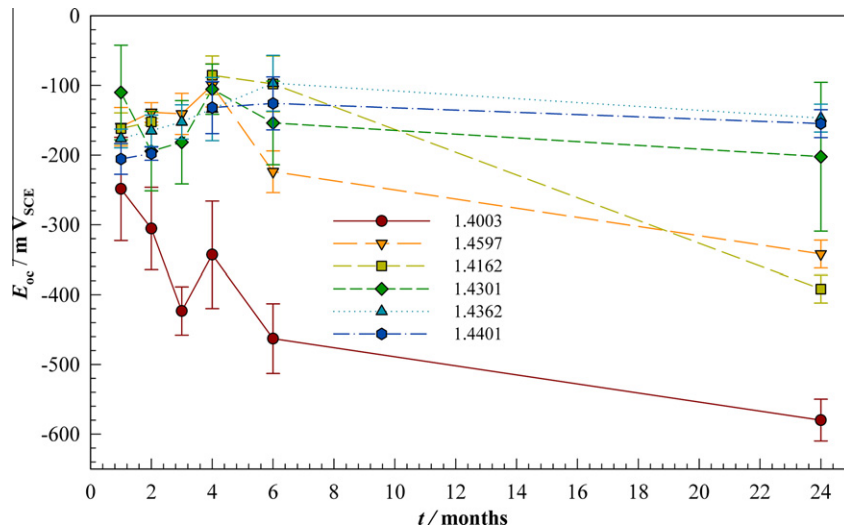


Fig. 5. A change of the open circuit potential (E_{oc}) of six tested steels embedded into mortar during 24 months of exposure to 3.5 wt.% NaCl solution.

constant. The first time constant, with phase maxima at 1 Hz, was attributed to the layer of corrosion products. The second, at 0.1 Hz, and the third, at 0.001 Hz, were attributed to the processes appearing at the pitted and passive area. The interfacial resistance of steel 1.4362 (Fig. 2c, Table 5) was significantly higher while the interfacial capacitance showed lower values compared to the other steel types even after 24 months of exposure. Such result may be an indicator of the better corrosion resistance of steel 1.4362, compared to both 1.4003 and 1.4162.

Results obtained by analysing EIS spectra were confirmed by visual analysis of specimens after the testing period of 24 months, Fig. 4a–c. Samples were open to allow visual inspection of steel surface and interfacial zone between the surface of the steel and mortar matrix. After 24 months of exposure, steel 1.4003 corroded extensively with corrosion pits formed and grouped throughout the surface of the steel (Fig. 4a). It can be seen that the corrosion

products, once formed in a significant amount, penetrated away from the surface of the steel through the mortar matrix and reached the concrete surface. This is in agreement with explanation of intermediate frequency impedance response obtained for this steel (Fig. 2a). In the case of steel 1.4162 (Fig. 4b), a localised dissolution of steel started in the crevice between impermeable seal and steel. Corrosion is localised, but the corrosion products did not form in a significant amount. In the case of steel 1.4362 (Fig. 4c), only a small pit formed on the steel surface, with no significant amount of corrosion products present at the steel/mortar interface.

3.2. Comparison of different types of stainless reinforcing steels

Open circuit potential and EIS spectra were periodically measured for six different types of steel, presented in Table 1, during

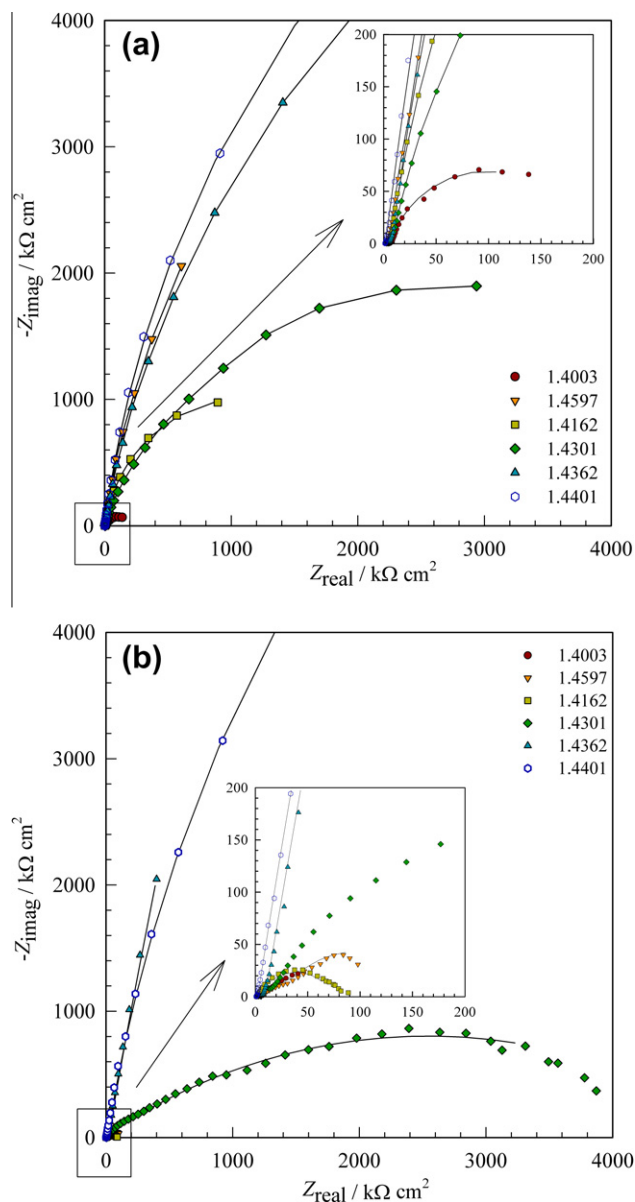


Fig. 6. Nyquist plots of mortar samples reinforced with different types of stainless reinforcing steel after 1 month of exposure (a) and 24 months of exposure (b) to 3.5 wt.% NaCl solution (experimental values given in dots, fitted in lines).

24 months of exposure to 3.5 wt.% NaCl solution, to compare and evaluate their long-term resistance to chloride-induced corrosion. Corrosion process was monitored non-destructively and was not interfered nor accelerated by an external current source, *i.e.* the results presented here represent evolution of natural chloride-induced corrosion process of steel embedded into poor quality mortar with insufficient thickness of mortar cover exposed to aggressive marine environment. Fig. 5 shows the representative results of E_{OC} time dependence, obtained from parallel measurements performed on 3 samples, for six different steel types embedded into mortar during 24 months of exposure to 3.5 wt.% NaCl solution. 1.4003 steel showed significantly lower potentials compared to the other steel samples what is in accordance with low corrosion resistance presented in Fig. 2a and Table 3. It can be seen that for steels with low Ni content (0.3–2%) and high Cr content (10–21%) change of potential towards more negative values occurred after 4 months of exposure. For steels with low to middle content of Ni (4–8%) and high content of Cr (17–21%)

change of potential towards more negative values occurred after 6 months of exposure, while for high Ni content (4–10%) and high Cr content (16–22%) steels the potentials showed stable values during the entire time of exposure. The change of E_{OC} towards more negative values can be considered as indicative of depassivation of steel and initiation of localized corrosion. There are some initiatives for quantitative evaluation of susceptibility to corrosion of black steel reinforcement in concrete according to values of the open circuit potential; however, these values are uncertain even for black steel reinforcement [31,32]. Therefore, only the trend of potential in time was taken into account in this study, with rapid decrease of potential being only indicative of destabilization or breakdown of the passive film and initiation of pitting corrosion, further supported with EIS results.

Fig. 6 shows Nyquist plots of mortar samples reinforced with different types of corrosion resistant steel after 1 month (a) and 24 months (b) of exposure to 3.5 wt.% NaCl solution. EIS parameters were obtained by fitting the impedance spectra presented in Fig. 6a and b to the equivalent electrical circuit presented in Fig. 3a and b. For comparison of corrosion resistances of studied types of steel, total resistance $R_t = R_1 + R_2$ was taken into account. Fig. 7 depicts the time dependence of the total resistance R_t of studied steels. It can be seen that higher alloyed steels show high R_t value even after long-term exposure to aggressive environment. Different types of steel can be listed in order depending on their corrosion resistance and the amount of Cr, Ni and Mo, from the least resistant to the most resistant. Steel 1.4003 with relatively low Cr content, low Ni and none Mo content showed poor corrosion resistance where pitting corrosion appeared after only 4 months of exposure to aggressive environment. Steel types with low Ni content but with high N and Mn content, 1.4597 and 1.4162, showed relatively good long-term corrosion resistance compared to steel 1.4003, even though their resistance was significantly lower than high Ni austenitic or duplex steels. An unexpected low corrosion performance of steel 1.4162 with relatively high PREN may be attributed to low Ni content. The addition of Ni to duplex stainless steels plays an important role in maintaining an austenite/ferrite balance, as austenite promoter and improver of pitting resistance [33]. On the other hand, Cr and Mo are enriched in ferrite phase as ferrite stabilizers. The addition of N has been proposed as economical alternative to Ni, due to its effective nickel-substituting potential for austenite formation. However, the addition of Mn to increase N solubility may result in formation of δ -ferrite and σ -phase that reduce the corrosion resistance. Lean duplex stainless steel 1.4162 represents such economical alternative to duplex stainless steels. It has high amount of Cr and lower amount of Ni but higher amount of N and Mn (Table 1). Although there are several investigations confirming its corrosion resistance in chloride media, its performance in chloride containing mortar has shown to be lower than 1.4301. The results presented in Figs. 5–7 have shown negative E_{OC} and lower total resistance from the beginning of the exposure to alkaline media. Even worst pitting corrosion performance after exposure of mortar embedded samples to chloride media has been obtained. Based on the literature data on N effect on the phase formation, it may be assumed that addition of Mn has induced negative effect on corrosion performance of steel 1.4162 in chloride containing alkaline media [10,33]. Alvarez et al. [9] have studied the corrosion performance of lean duplex stainless steel 1.4482 in simulated concrete pore solution. Steel 1.4482 that has similar chemical composition like 1.4162, low-Ni, high-Mn, has shown similar performance to 1.4307 in alkaline media containing chloride ions. In carbonated chloride containing simulated pore solutions this steel shows almost none passive region at the anodic polarization curves. Pitting attack appeared without the need of reaching high anodic potentials, while repassivation of pits during the reverse scan did not oc-

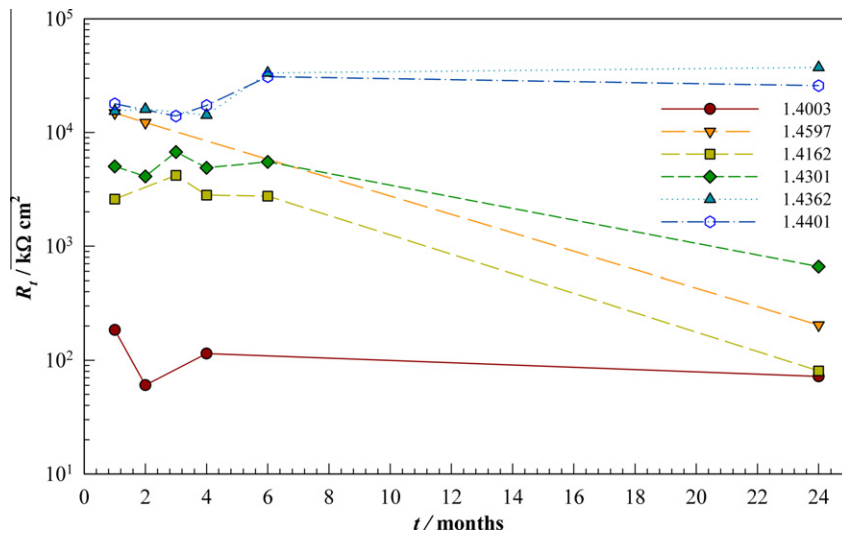


Fig. 7. The time dependence of total resistance (R_t) of six tested steels embedded into mortar during 24 months of exposure to 3.5 wt.% NaCl solution.

cur. The attack in a shape of a numerous small pits was attributed to the lower Cr content of the passive layer in the experimental conditions applied and characterised as less dangerous morphology compared to the large deep pits appearing at the 1.4307. A microstructural factor that is, besides chemical composition, also controlling the corrosion of duplex steel was underlined. Microstructural analysis revealed selective dissolution of austenite phase as an onset of pitting that was attributed to the presence of Mn as the austenite stabilizer instead of Ni.

Austenitic stainless steel 1.4301, has shown a good corrosion resistance with high total resistance values in the initial phase. However, after 24 months steel 1.4301 has shown a medium corrosion resistance compared to Mo containing austenitic stainless steel 1.4401. Anyhow, in this study, the very good corrosion performance of stainless steels grade 1.4301 and 1.4401 has been confirmed; therefore they were used as reference for comparison with economically more acceptable, low nickel austenitic or duplex stainless steels. It can be seen that duplex steel 1.4362 with medium Ni content showed very good corrosion resistance, somewhat better than austenitic steel 1.4401 with high Ni content. Very good corrosion resistance of this steel could be attributed to good protective properties of the passive film, enriched with Cr, Ni and Mo. Freire et al. [14] have shown that the passive film on 1.4301 and 1.4401 exposed to alkaline media becomes enriched with chromium with simultaneous decrease of magnetite content as the pH is lowered from 13 to 9. Addari et al. [16] has shown that passive film at the surface of ferritic and duplex steels becomes enriched with chromium oxy-hydroxyde with time of exposure to alkaline media, while passive film on austenitic steel becomes strongly enriched in nickel hydroxide. The study on effect of Ni on properties of stainless steels has revealed that enhancement of Ni content results in formation of more protective passive film with increasing pitting resistance in chloride environment [15,33]. Research of duplex steels has revealed the presence of molybdates at the passive film surface, as adsorbed intermediate, that have a stabilizing effect on the passive film that is thinner but with enhanced Cr/Fe ratio, which could be an explanation of their good corrosion resistance, regardless the lower amount of Ni [14].

As more economic substitute austenitic stainless steel 1.4597 was studied showing a corrosion resistance comparable to 1.4301 steel in chloride containing simulated pore solution [10,11]. It was shown that passive film on steel 1.4597 exposed

to simulated pore solution has lower Cr-content compared to 1.4301. On the other hand passive film at the steel 1.4597 surface contains poorly-protective Mn oxides, owing to the high percentage of Mn in the steel bulk. Long-term corrosion testing setup utilized in our studies has revealed (Fig. 7) somewhat lower corrosion performance of steel 1.4597 compared to 1.4301, showing the onset of pitting after only 4 month, which might be more realistic compared to the measurements conducted in the simulated pore solution after the short immersion times.

Duplex stainless steels 1.4362 have shown good corrosion performance during the 24 month exposure to the corrosive conditions of the mortar embedded samples. Extensive study of Moser et al. [8] has shown very good corrosion performance of 1.4362 and 1.4462. One of the first studies on the corrosion resistance of alternative stainless reinforcing steel, done by Blanco et al. [12] has shown very good corrosion resistance of duplex stainless steel 1.4462, comparable or even better than steels 1.4301 and 1.4401. Stainless steel 1.4362 has shown better corrosion performance compared to 1.4301 but somewhat lower compared to excellent performance shown by 1.4462 [9]. Selective dissolution was observed on 1.4362 in carbonated solution with high concentration of Cl^- with localized attack induced by selective dissolution of ferrite phase. Dissolution of ferrite phase in tested conditions was ascribed to the enhanced corrosion resistance of austenite phase due to the increased content of austenite stabilizer Ni. On the other hand, significantly lower content of ferrite stabilizer Mo may also be a cause of the ferrite phase lower performance. Usually, selective dissolution is associated with changes in chemical composition austenite phase. However, phase attack may vary dependant on the corrosive conditions and the onset of corrosion is dependent on the corrosion resistance of the weakest phase. Selective dissolution of ferrite phase during anodic polarization test of duplex 1.4362 exposed to alkaline media containing chloride was reported by Alvarez et al. [9]. Author stresses out the importance of microstructure in development of localized attack.

4. Conclusions

The paper presents an analysis of long – term corrosion behaviour of six stainless reinforcing steels (1.4003, 1.4597, 1.4162, 1.4362, 1.4301 and 1.4401) that had been embedded in mortar, exposed to chloride media and monitored during a period of 2 years.

Electrochemical impedance spectroscopy results and E_{OC} values after different times of exposure enabled differentiation of two phases of corrosion behaviour: (i) passive or pitting initiation phase (ii) pitting propagation phase. The interfacial behaviour of steels was discussed within the frames of physical meaning of equivalent electrical circuit used and the parameters obtained by the fitting procedure. The enhancement of the charge transfer resistance and double layer capacitance with time was attributed to the growth of the passive film at the steel surface during the passivity period. Sudden decrease of the charge transfer resistance accompanied with increase of the double layer capacitance was associated with pitting onset and accumulation of the corrosion products at the pitted sites.

Duplex steel 1.4362 showed very good corrosion performance similar to common austenitic steel 1.4401. Superior corrosion performance of this steel was attributed to the good protective properties of the passive film, enriched with Cr, Ni and Mo. Steel types with low Ni content but with high N and Mn content, 1.4597 and 1.4162, show good long-term corrosion performance compared to steel 1.4003, but relatively lower corrosion resistance when compared to common austenitic steels, 1.4401 and 1.4301.

Acknowledgements

This research was funded by scientific Projects 082-0822161-2159 and 125-0822161-2982, both funded by Croatian Ministry of Education, Science and Sport, and partly by European FP6 Project TST5-CT-2006-031272. Authors would like to thank companies Roldan S.A. (ACERINOX group), Swiss Steel AG and Outokumpu GesmbH for providing steel samples used in this research.

References

- [1] L. Bertolini, B. Elsener, P. Pedeferra, R.B. Polder, Corrosion of Steel in Concrete Prevention, Diagnosis, Repair, Wiley, VCH, Weinheim, 2004.
- [2] U. Nürnberger, Stainless Steel in Concrete – State of the Art Report, European Federation of Corrosion by the Institute of Materials, London, UK, 1996.
- [3] C.M. Abreu, M.J. Cristóbal, R. Losada, X.R. Nóvoa, G. Pena, M.C. Pérez, High frequency impedance spectroscopy study of passive films formed on AISI 316 stainless steel in alkaline medium, *J. Electroanal. Chem.* 572 (2004) 335–345.
- [4] L. Veleva, M. Alpuche-Aviles, M.K. Graves-Brook, D. Wipf, Comparative cyclic voltammetry and surface analysis of passive films grown on stainless steel 316 in concrete pore model solutions, *J. Electroanal. Chem.* 537 (2002) 85–93.
- [5] L. Veleva, M. Alpuche-Aviles, M. Graves-Brook, D. Wipf, Voltammetry and surface analysis of AISI 316 stainless steel in chloride-containing simulated concrete pore environment, *J. Electroanal. Chem.* 578 (2005) 45–53.
- [6] The concrete society, Guidance on the use of stainless steel reinforcement, Report of a Concrete Society Steering Committee, Technical Report Number 51, 1998.
- [7] G. Gedge, Structural uses of stainless steel – buildings and civil engineering, *J. Constr. Steel Res.* 64 (2008) 1194–1198.
- [8] R.D. Moser, P.M. Singh, L.F. Kahn, K.E. Kurtis, Chloride-induced corrosion resistance of high-strength stainless steels in simulated alkaline and carbonated concrete pore solutions, *Corros. Sci.* 57 (2012) 241–253.
- [9] S. Alvarez, A. Bautista, F. Velasco, Corrosion behaviour of corrugated lean duplex stainless steels in simulated concrete pore solutions, *Corros. Sci.* 53 (2011) 1748–1755.
- [10] A. Bautista, G. Blanco, F. Velasco, Corrosion behaviour of low-nickel austenitic stainless steels reinforcements: a comparative study in simulated pore solutions, *Cem. Concr. Res.* 36 (2006) 1922–1930.
- [11] A. Bautista, G. Blanco, F. Velasco, A. Gutiérrez, L. Soriano, F.J. Palomares, H. Takenouti, Changes in the passive layer of corrugated austenitic stainless steel of low nickel content due to exposure to simulated pore solutions, *Corros. Sci.* 51 (2009) 785–792.
- [12] G. Blanco, A. Bautista, H. Takenouti, EIS study of passivation of austenitic and duplex stainless steels reinforcements in simulated pore solutions, *Cem. Concr. Comp.* 28 (2006) 212–219.
- [13] H. Luo, C.F. Dong, X.G. Li, K. Xiao, The electrochemical behaviour of 2205 duplex stainless steel in alkaline solutions with different pH in the presence of chloride, *Electrochim. Acta* 64 (2012) 211–220.
- [14] L. Freire, M.A. Catarino, M.I. Godinho, M.J. Ferreira, M.G.S. Ferreira, A.M.P. Simões, M.F. Montemor, Electrochemical and analytical investigation of passive films formed on stainless steels in alkaline media, *Cem. Concr. Comp.* 34 (2012) 1075–1081.
- [15] C. Abreu, M. Cristóbal, R. Losada, X. Nóvoa, G. Pena, M. Perez, The effect of Ni in the electrochemical properties of oxide layers grown on stainless steels, *Electrochim. Acta* 51 (2006) 2991–3000.
- [16] D. Addari, B. Elsener, A. Rossi, Electrochemistry and surface chemistry of stainless steels in alkaline media simulating concrete pore solutions, *Electrochim. Acta* 53 (2008) 8078–8086.
- [17] C. Olsson, Passive films on stainless steels – chemistry, structure and growth, *Electrochim. Acta* 48 (2003) 1093–1104.
- [18] D. Trejo, P. Monteiro, Corrosion performance of conventional (ASTM A615) and low-alloy (ASTM A706) reinforcing bars embedded in concrete and exposed to chloride environments, *Cem. Concr. Res.* 35 (2005) 562–571.
- [19] J. Scully, M. Hurley, Investigation of the Corrosion Propagation Characteristics of New Metallic Reinforcing Bars, Virginia Transportation Research Council, Charlottesville, VA, 2007.
- [20] M.C. García-Alonso, M.L. Escudero, J.M. Miranda, M.I. Vega, F. Capilla, M.J. Correia, M. Salta, A. Bennani, J.A. González, Corrosion behaviour of new stainless steels reinforcing bars embedded in concrete, *Cem. Concr. Res.* 37 (2007) 1463–1471.
- [21] M.C. García-Alonso, J.A. González, J. Miranda, M.L. Escudero, M.J. Correia, M. Salta, A. Bennani, Corrosion behaviour of innovative stainless steels in mortar, *Cem. Concr. Res.* 37 (2007) 1562–1569.
- [22] E.C. Paredes, A. Bautista, S.M. Alvarez, F. Velasco, Influence of the forming process of corrugated stainless steels on their corrosion behaviour in simulated pore solutions, *Corros. Sci.* 58 (2012) 52–61.
- [23] C. Andrade, M. Keddad, X. Nóvoa, M. Perez, C. Rangel, H. Takenouti, Electrochemical behaviour of steel rebars in concrete: influence of environmental factors and cement chemistry, *Electrochim. Acta* 46 (2001) 3905–3912.
- [24] L. Valek, S. Martinez, D. Mikulic, I. Brnardic, The inhibition activity of ascorbic acid towards corrosion of steel in alkaline media containing chloride ions, *Corros. Sci.* 50 (2008) 2705–2709.
- [25] A. Bautista, A. Gonzalez, Centeno, G. Blanco, S. Guzman, Application of EIS to the study of corrosion behaviour of sintered ferritic stainless steels before and after high-temperature exposure, *Mater. Charact.* 59 (2008) 32–39.
- [26] B. Diaz, L. Freire, P. Merino, X. Nóvoa, M. Perez, Impedance spectroscopy study of saturated mortar samples, *Electrochim. Acta* 53 (2008) 7549–7555.
- [27] D.A. Koleva, J.H.W. de Wit, K. van Breugel, L.P. Veleva, E. van Westing, O. Copuroglu, A.L.A. Fraaij, Correlation of microstructure, electrical properties and electrochemical phenomena in reinforced mortar. Breakdown to multi-phase interface structures. Part II: Pore network, electrical properties and electrochemical response, *Mater. Charact.* 59 (2008) 801–815.
- [28] D.A. Koleva, K. van Breugel, J.H.W. de Wit, E. van Westing, O. Copuroglu, L. Veleva, A.L.A. Fraaij, Correlation of microstructure, electrical properties and electrochemical phenomena in reinforced mortar. Breakdown to multi-phase interface structures. Part I: Microstructural observations and electrical properties, *Mater. Charact.* 59 (2008) 290–300.
- [29] M. Farcas, N.P. Cosman, D.K. Ting, S.G. Roscoe, S. Omanovic, A comparative study of electrochemical techniques in investigating the adsorption behaviour of fibrinogen on platinum, *J. Electroanal. Chem.* 649 (2010) 206–218.
- [30] F. Mansfeld, Electrochemical impedance spectroscopy (EIS) as a new tool for investigating methods of corrosion protection, *Electrochim. Acta* 35 (1990) 1533–1544.
- [31] C. Andrade, C. Alonso, J. Gulikers, R. Polder, R. Cigna, O. Vennesland, M. Salta, A. Raharinaivo, B. Elsener, Recommendations of RILEM TC-154-EMC: “Electrochemical techniques for measuring metallic corrosion” test methods for on-site corrosion rate measurement of steel reinforcement in concrete by means of the polarization resistance method, *Mater. Struct.* 37 (2004) 623–643.
- [32] B. Elsener, C. Andrade, J. Gulikers, R. Polder, M. Raupach, Half-cell potential measurements – potential mapping on reinforced concrete structures, *Mater. Struct.* 36 (2003) 461–471.
- [33] J.H. Potgieter, P.A. Olubambi, L. Cornish, C.N. Machio, El-Sayed M. Sherif, Influence of nickel additions on the corrosion behaviour of low nitrogen 22% Cr series duplex stainless steels, *Corros. Sci.* 50 (2008) 2572–2579.